Atmos. Meas. Tech. Discuss., 6, 2151–2181, 2013
www.atmos-meas-tech-discuss.net/6/2151/2013/
doi:10.5194/amtd-6-2151-2013

Atmospheric Measurement Techniques Discussions

Performance of diethylene glycol based particle counters in the sub 3 nm size range

D. Wimmer[1,*], K. Lehtipalo[2,3], A. Franchin[2], J. Kangasluoma[2], F. Kreissl[1], A. Kürten[1], A. Kupc[4], A. Metzger[1], J. Mikkilä[3], T. Petäjä[2], F. Riccobono[5,], J. Vanhanen[3], M. Kulmala[2], and J. Curtius[1]**

[1]Institute for Atmospheric and Environmental Sciences, Goethe University of Frankfurt, Frankfurt am Main, Germany
[2]Department of Physics, University of Helsinki, Helsinki, Finland
[3]Airmodus, Ltd, Gustaf Hällströmin katu 2a, 00560 Helsinki, Finland
[4]University of Vienna, Faculty of Physics, Vienna, Austria
[5]Laboratory of Atmospheric Chemistry, Paul Scherrer Institute, Villigen, Switzerland
[*]now at: Department of Physics, University of Helsinki, Helsinki, Finland
[**]now at: Joint Research Centre, European Commission, 21027 Ispra, Italy

Received: 17 January 2013 – Accepted: 14 February 2013 – Published: 26 February 2013

Correspondence to: J. Curtius (curtius@iau.uni-frankfurt.de)

Published by Copernicus Publications on behalf of the European Geosciences Union.

Abstract

When studying new particle formation, the uncertainty in determining the "true" nucleation rate is considerably reduced when using Condensation Particle Counters (CPCs) capable of measuring concentrations of aerosol particles at sizes close to or even at the critical cluster size (1–2 nm). Recently CPCs, able to reliably detect particles below 2 nm in size and even close to 1 nm became available. The corrections needed to calculate nucleation rates are substantially reduced compared to scaling the observed formation rate to the nucleation rate at the critical cluster size. However, this improved instrumentation requires a careful characterization of their cut-off size and the shape of the detection efficiency curve because relatively small shifts in the cut-off size can translate into larger relative errors when measuring particles close to the cut-off size.

Here we describe the development of two continuous flow CPCs using diethylene glycol (DEG) as the working fluid. The design is based on two TSI 3776 counters. Several sets of measurements to characterize their performance at different temperature settings were carried out. Furthermore two mixing-type Particle Size Magnifiers (PSM) A09 from Airmodus were characterized in parallel. One PSM was operated at the highest mixing ratio (1 L min^{-1} saturator flow), and the other was operated in a scanning mode, where the mixing ratios are changed periodically, resulting in a range of cut-off sizes. Different test aerosols were generated using a nano-Differential Mobility Analyzer (nano-DMA) or a high resolution DMA, to obtain detection efficiency curves for all four CPCs. One calibration setup included a high resolution mass spectrometer (APi-TOF) for the determination of the chemical composition of the generated clusters. The lowest cut-off sizes were achieved with negatively charged ammonium sulphate clusters, resulting in cut-offs of 1.4 nm for the laminar flow CPCs and 1.2 and 1.1 nm for the PSMs. A comparison of one of the laminar-flow CPCs and one of the PSMs measuring ambient and laboratory air showed good agreement between the instruments.

AMTD
6, 2151–2181, 2013

1 Introduction

Roughly 50 % of the global Cloud Condensation Nuclei (CCN) are thought to originate from secondary aerosol production in the atmosphere (Merikanto et al., 2009). Therefore one major topic in atmospheric sciences is the detailed study of nucleation processes. As atmospheric new particle formation happens in the size range below 2 nm, there has been a growing demand to extend the range, where direct measurements are possible also, to that size range. The lower size limit of a condensation particle counter (CPC) is generally described by the diameter at which the counter still detects half of the particles. This diameter is called cut-off diameter or d_{50}. Using condensation particle counters with low cut-off sizes enables detecting particles right after they are formed, even when the initial growth rate is slow. This also allows to obtain information on the particle formation rate close to or even at the critical cluster size (Kulmala et al., 2012), without the need to scale down the measurement data of CPCs with larger cut-off sizes, by using assumptions about the particle growth rate and the loss mechanisms. It has been proposed (Sipilä et al., 2010) that the inability of reproducing atmospheric nucleation rates in the laboratory could be explained by the slow growth of particles together with the relatively large cut-off sizes of the instrumentation used in most experiments.

Condensation particle counters are the most commonly used instruments for measuring the total particle number concentration in the sub-micrometer range (McMurry, 2000). The working principle of a condensation particle counter is to expose the aerosol sample to a supersaturated vapour, which can condense on the particles, thereby making them large enough to be detected optically. At least three different methods have been used for creating the required supersaturation: adiabatic expansion, thermal diffusion in a laminar flow or mixing of two flows with different thermodynamic properties.

The overall detection efficiency of a CPC depends both on the losses of particles inside the instrument as well as on the activation probability of the particles (Stolzenburg and McMurry, 1991).

AMTD
6, 2151–2181, 2013

$$\eta_{\mathrm{CPC}(D_\mathrm{p})} = \eta_{\mathrm{sam}(D_\mathrm{p})} \cdot \eta_{\mathrm{act}(D_\mathrm{p})} \cdot \eta_{\mathrm{det}(D_\mathrm{p})} \quad (1)$$

where η_{sam} is the sampling efficiency which is defined as the ratio of particle concentrations exiting the capillary and the concentrations extracted from the sample flow; η_{act} is defined as the activation efficiency; and η_{det} is defined as the detection efficiency of the particles in the optics (also called counting efficiency).

The activation probability, in turn, mainly depends on the supersaturation of the condensing vapour which the particles are exposed to and also on the activating vapour. Besides the size of the particles, i.e. their surface curvature (Kelvin effect), their chemical composition and their charging state can have an influence on their activation (Kulmala et al., 2007b; Winkler et al., 2008). The cut-off size of a CPC can be lowered mainly by increasing the supersaturation, but also to some extent by minimizing the diffusional losses of particles inside the instrument. The first CPCs designed specifically for ultrafine particles were developed in the 1990s with a cut-off size around 3 nm (Stolzenburg and McMurry, 1991). The demand to measure even smaller particles – mainly to study atmospheric nucleation – has led to further CPC development and by now several different instruments have been reported to measure in the sub-3 nm size range (Seto et al., 1997; Sgro and Fernandez de la Mora, 2004; Mordas et al., 2005; Kulmala et al., 2007a; Sipilä et al., 2008, 2009; Iida et al., 2009; Lehtipalo et al., 2009, 2010; Saghafifar et al., 2009; Vanhanen et al., 2011).

2 General considerations

One limiting factor in lowering the cut-off diameter of a CPC is homogeneous nucleation inside the instrument. If the saturation ratio is too high, homogeneous nucleation of the working fluid can occur, which leads to a higher count rate in the CPC due to the internally produced particles. Iida et al. (2009) evaluated different working fluids for CPCs and showed that by selecting a working fluid with high surface tension, but

AMTD
6, 2151–2181, 2013

low enough saturation vapour pressure one can achieve high supersaturations without considerable homogeneous nucleation. In that study, diethylene glycol was identified as a fluid with very favorable properties and it has been demonstrated that it can be used to activate particles even close to 1 nm (Jiang et al., 2011b; Vanhanen et al., 2011).

The calibration of a CPC requires being able to produce a monodisperse aerosol with known size, chemical composition and charging state, which is not straightforward in the size range below 3 nm. CPCs are calibrated by using an aerosol generator and after that, a Differential Mobility Analyzer (DMA) where the aerosol is classified according to the electrical mobility of the particles. As a reference instrument usually an electrometer is used. One major topic in aerosol nucleation studies is the question how far the nucleation process is affected by the presence of ions (Kirkby et al., 2011). In the atmosphere ions are always present and therefore the measured formation rates will include both the neutral and the charged component if no ion filter is used in front of the CPCs. Therefore, it is useful to calibrate CPCs with charged particles of both polarities, but calibration measurements using neutral particles would also be desirable. Thus charged particles of different compositions are normally used for calibrating CPCs.

Measurements in the sub-3 nm size range need to achieve a stable and sufficient concentration of aerosols for each selected size. Furthermore, significant diffusional losses have to be considered. Even if one manages to produce large amounts of 1 nm particles, a sufficient concentration needs to reach the aerosol counters after charging and transfer through the DMA.

Here we aim to characterize 4 diethylene glycol-based CPCs: 2 laminar flow DEG CPCs (modified TSI 3776) and 2 mixing-type Particle Size Magnifiers (Airmodus A09 PSM), and the focus is on the validation of their performance in the sub-3 nm size range through precise laboratory calibrations. In addition, two of the instruments of different type were inter-compared while measuring ambient air. All of the 4 instruments

AMTD
6, 2151–2181, 2013

were used in the CLOUD experiments at CERN and the calibration data is crucial for evaluating and understanding their performance during the experiments.

3 Experimental description

3.1 The DEG CPCs

Diethylene glycol is very well suited for activating aerosol particles smaller than 3 nm, but as its absolute saturation vapour pressure at typical saturator temperatures is low the particles grow only to sizes of about 90–100 nm and are thus too small for direct optical detection (Iida et al., 2009; Vanhanen et al., 2011). This means that a special setup consisting of two growth stages is required. In the first stage the particles are activated and grown by DEG, in the second stage they grow further and the actual counting of the particles takes place. For the second stage a commercial CPC can be used which will be termed the "booster" CPC in the following, according to the nomenclature given by Iida et al. In the work presented here, two butanol based CPCs a TSI 3776 (d_{50} = 2.5 nm), a TSI 3010 (d_{50} = 10 nm) and an isopropanol-based TSI 3007 (d_{50} = 10 nm) have been used as booster CPCs. The total flow through the DEG stage is set to 0.3 L min^{-1}, but the booster can have a higher inlet flow rate. In this case an additional adjustable dilution flow after the DEG stage is required.

Iida et al. (2009) used a total inlet flow rate into the CPC of 0.3 L min^{-1}. The condenser temperature was at 10 °C and the saturator temperature was set to 50 °C. The wick that is installed inside the saturator was replaced by a 14 × 14 cm cellulose sheet. However, in the work presented here two standard TSI 3776 ultrafine butanol CPCs were modified: after removing the wick, a cellulose filter was wrapped around a perforated stainless steel tube housed in the saturator part of the CPC. Since the TSI software does not allow for controlling the saturator temperature to values larger than 50 °C, an additional temperature control was installed. It consists of a Pt1000 attached directly outside the saturator block and a PID (Proportional-Integral-Derivative) heat

AMTD
6, 2151–2181, 2013

control unit (EZ-Zone, PM 6CICK-2AAAAAA). The optics part of the CPC was removed and instead, an adapter was attached to the outlet of the condenser in order to connect it to a booster CPC.

Test measurements were performed to determine the highest saturator temperature where no homogeneous nucleation occurs while having the condenser at a fixed temperature of 10 °C. This saturator temperature was found to be 52 °C. One of the DEG CPCs was always operated with these settings and is termed DEG CPC 1. During these measurements, a high efficiency particle filter was installed at the inlet of the CPCs (using laboratory air as carrier gas) while stepping up the saturator temperature. With the temperatures of 10 and 52 °C the homogeneous nucleation was about 0.01–0.02 $cm^{-3} min^{-1}$.

For the second setup the same modifications were performed, but with two additional changes. The flow rate through the aerosol capillary was increased (from 40–50 to 90–100 $cm^3 s^{-1}$), which allowed raising the saturator temperature to 55 °C before substantial homogeneous nucleation occurred. This was verified by applying the same procedure as mentioned before and the same particle formation rate by homogeneous nucleation was achieved. Another change was made by implementing a needle valve and an external pump (see Fig. 1). Thereby, the inlet flow rate of the CPC could be increased up to 1.8 $L min^{-1}$. In the following, this setup will be referred to as DEG CPC 2.

Details for the systems, displaying the flow schemes and temperatures are shown in Fig. 1. Labels in green font represent the working conditions for the DEG CPC 1; magenta represents the settings used for the DEG CPC 2. Similar modifications were reported by Kuang et al. (2011). They showed that with these modifications the detection efficiencies of the CPCs were improved significantly, when using negatively charged sodium chloride (NaCl) as a test aerosol.

3.2 The particle size magnifier

The Particle Size Magnifier (PSM; Airmodus A09) is a mixing-type condensation particle counter, in which the supersaturation required for activating particles is achieved by

AMTD
6, 2151–2181, 2013

turbulently mixing the sample with clean air saturated with diethylene glycol. A regular commercial CPC (TSI 3772 or TSI 3010) was used for further growing and counting the activated particles. Details of the instrument are described by Vanhanen et al. (2011). The cut-off size of the PSM can be varied by changing the mixing ratio of the saturator and sample flow rate, which determines the supersaturation achieved in the mixing section. Therefore, using the PSM in a scanning mode, also information about the particle size distribution can be obtained. The relationship between the mixing ratio and activation diameter of particles is based on laboratory calibrations. Figure 2 shows how the detection efficiency of differently sized negative ammonium sulphate clusters change when varying the PSM saturator flow rate. Particles above 2 nm in diameter are detected already with very small saturator flow rates (mixing ratio < 0.07), whereas 1.2 nm clusters require a mixing ratio higher than 0.22 before they are detected. The ammonium sulphate clusters were produced with the setup described in Fig. 3 (see next Sect. 3.3).

3.3 Generation of test aerosols

The main focus of this work is to characterize and compare the detection efficiencies of the DEG CPCs and the PSMs. Therefore, detailed calibration measurements were carried out using various methods for providing monodisperse aerosol particles in the size range between 1 and 10 nm.

The first setup is shown in Fig. 3a, where a nano-DMA (Grimm Aerosol Technik, S-DMA, 55–100) was used for size selecting the generated aerosol particles. In this case the DMA was running in a closed loop arrangement with a sheath air flow rate of 20 L min^{-1}. Three different types of aerosol generators were used in this configuration. These are; (a) a tungsten oxide generator (Grimm Aerosol Technik, NANO WO_x Generator, 7.860), (b) a tube furnace using NaCl (Scheibel and Porstendörfer, 1983) and (c) a sulphuric acid particle generator (Middlebrook et al., 1997). The sulphuric acid particle generator consists of a small heated quartz glass tube containing a ceramic vessel filled with sulphuric acid (Carl Roth GmbH + Co. KG, 95 %). The temperatures

AMTD
6, 2151–2181, 2013

of the heater were varied between 55 and 77 °C. Particle-free air from the laboratory was used as carrier gas for all the generators used in this configuration.

The high resolution DMA (Herrmann et al., 2000) was operated in two different modes. The first one is shown in Fig. 3b, where the high resolution DMA was running in an open loop arrangement and the DEG CPC 1 was calibrated against an electrometer. In the second mode (Fig. 3c), the high resolution DMA was operated in a closed loop arrangement, while one DEG CPC and one PSM at a time were calibrated in parallel against an electrometer. All 4 instruments were calibrated using this setup. A high resolution mass spectrometer capable of analyzing the composition of the clusters. (Atmospheric Pressure Interface – Time of flight APi-TOF, Junninen et al., 2010) was measuring in parallel to verify that the composition of the aerosol was free of impurities and did not change during the calibration measurements. By using pure nitrogen as carrier gas (5.0), the aerosol sample was observed to be bisulphate clusters with only a few contaminant substances at low levels, while contaminant levels were considerably higher when filtered lab air was used. Since no direct measurement of the high-resolution DMA sheath gas flow was available, ions from an electrospray source with known electrical mobility were used to calibrate the voltage-mobility relation flow prior to each measurement (Fernandez de la Mora et al., 2005).

4 Results

4.1 Cut-off measurements

In the following, the results of the cut-off measurements are presented. The diameters reported here are electrical mobility equivalent diameters, because the DMA measurement principle is based on electrical mobility. When the mobility is converted into a diameter, the use of the mobility diameter is most direct, while the conversion to a mass equivalent diameter introduces additional uncertainties (Ki Ku and Fernandez de la Mora, 2009; Ehn et al., 2011).

AMTD
6, 2151–2181, 2013

The detection efficiencies shown in the following were derived from the ratio of the concentrations measured by a CPC and an electrometer, which was normalized to 1 at larger sizes to account for small differences in the set-ups. Two different electrometers (Grimm Aerosol Technik, FCE – Grimm model 5.705 and TSI model 3068B) were used as reference instruments and an inter-comparison showed that they yielded mean measured concentrations for a certain diameter between 0.5–1 %. The concentrations measured by the electrometer were corrected for the offset, by setting the voltage at the center electrode of the DMA to zero, which prevents particles from reaching the exit. Since the offset can vary with time, the zero measurement was done regularly. The concentrations were also corrected for diffusional losses (Chen and Pui, 2001) for each CPC/electrometer individually since they have different inlet flow rates. All the fitting curves for the counting efficiencies shown in the following are based on the function proposed by Wehner et al. (2011) except for Fig. 7a. The maximum error in the selected mobility diameter using the nano-DMA was 10 % at 1 nm, where the high resolution DMA had a resolution of about 20 (Jiang et al., 2011a).

Figure 4 shows the detection efficiency as a function of the saturator temperature for the DEG CPC 1. For each setting the condenser temperature was kept constant at 10 °C, whereas the saturator temperature was varied between 40 °C (dark blue line) and 55 °C (red line). The plot clearly shows that the detection efficiencies of the DEG CPC 1 vary with the temperature difference between saturator and condenser. For the smallest temperature difference between the saturator and the condenser, the d_{50} was found to be 2.7 nm. For the temperature of 52 °C, the 50 % detection efficiency was 2.0 nm and for 55 °C 1.8 nm. These two temperature settings are used for the DEG CPC 1 and 2 respectively, but the highest temperature difference could only be realized with the higher capillary flow rate while avoiding significant homogeneous nucleation. The fact that the curves shown in Fig. 4 reach different plateau values is most likely due to internal losses inside the DEG CPC 1 and 2 and to incomplete activation of particles which travel through regions of the condenser with lower saturation ratio (Stratmann et al., 1994).

AMTD
6, 2151–2181, 2013

Figure 5 shows the detection efficiency of the DEG CPC 1 applying the methods of generating test-aerosols according to Fig. 3a and b. The circles show the measurements performed with the nano-DMA and the triangles with the high resolution DMA (in the open loop configuration). By using this configuration, a d_{50} of 2.0 nm was achieved. The results of the measurements performed providing sulphuric acid particles (according to set-up Fig. 3a) are shown in Fig. 6. Here one data point at 1.7 nm is higher than expected and similar calibrations did not reproduce this high point, therefore it is regarded as an experimental outlier. A d_{50} of 2.0 nm was achieved also for sulphuric acid test aerosol.

Figure 7a shows a comparison of the detection efficiencies for PSM 1 and 2 as well as DEG CPC 1 and 2 using the setup from Fig. 3c. The PSM 1 was set to the highest saturator flow, so it was operating at the lowest cut-off diameter, whereas the PSM 2 was in scanning mode and the results shown here are achieved, by using the channel with the highest mixing ratio. The figure shows the results for a set of measurements where negatively charged ammonium sulphate particles were used as test aerosol; here a sigmoid fit function was applied, since the fit proposed by Wehner et al. (2011) did not represent the data properly. Surprisingly, the cut-off of the DEG CPC 1 (1.4 nm) seems to be considerably lower (by 0.6 nm) than shown in Fig. 5 whereas the DEG CPC 2 has a 50 % detection efficiency of 1.3 nm. The fact that the cut-off of the DEG CPC 1 is significantly shifted towards lower sizes compared to the calibration measurements using tungsten oxide and sulphuric acid particles is unexpected, since the results for the other measurements all showed a cut-off diameter of $\cong$ 2 nm. Nevertheless, similar results for the d_{50} (1.4 nm) for negatively charged ammonium sulphate particles are reported by Iida et al. (2009). The PSMs here also show the lowest cut-offs that have been achieved throughout the measurements and have a d_{50} detection efficiency of 1.1/1.2 nm.

Figure 7b shows the detection efficiencies for both PSM 1/2 and DEG CPC 2 using the setup Fig. 3c. The aerosol used here was positively charged ammonium sulphate. According to these measurements the DEG CPC 2 had a 50 % detection efficiency at

AMTD
6, 2151–2181, 2013

1.7 nm. The PSMs here agree nicely with each other. Both have a cut-off of 1.6 nm, which were the highest cut-offs that have been measured with the PSMs within this study.

Figure 7c shows the detection efficiencies for both PSM 1/2 and DEG CPC 1/2 applying the setup shown in Fig. 3c where negatively charged sodium chloride particles were generated. This data shows 50 % detection efficiencies of 1.7 nm for the DEG CPC 2 and 2 nm for the DEG CPC 1 respectively. The cut-off for both PSMs for sodium chloride was 1.2 nm.

One reason for the differences in the cut-off sizes of the CPCs for the different test aerosols might be the following: when using an APi-TOF in parallel, to measure the cluster composition, we found out that, if the aerosol sample and the measurement setup is not cleaned carefully it will contain molecular impurities, which seem to affect the measurement at sizes smaller than about 1.7 nm. Especially when generating positively charged aerosol particles, it turned out that it was impossible to produce a completely clean test aerosol without organic impurities in our set up, which could explain the higher cut-off size (by 0.5 nm) for positive ammonium sulphate. The effect of a lower detection efficiency for positively charged clusters, has been shown by various other studies, even for different working fluids (Winkler et al., 2008; Iida et al., 2009; Kuang et al., 2011). One possible explanation might be that the organic vapours that are mostly used as working fluids, are positively charged and therefore more likely bind with negatively charged clusters. Therefore clusters with higher organic impurity are more difficult to being activated. Another explanation could be that in the positive polarity where the ions produced in the charger are bigger, they can have an influence on the detection efficiency curves, as their activation properties are different than the sample ions (Sipilä et al., 2009; Kangasluoma et al., 2013). The overall question comes up, if the lower activation efficiency for positively charged aerosols is due to the charge sign or due to the fact that in the positive case the organic contribution is always higher than in the negative case. Whereby these two effects are very likely not to be completely de-coupled from each other.

AMTD
6, 2151–2181, 2013

The 50 % detection efficiencies are summarized in Table 1 and the overall results indicate that the effect of the aerosol type on the detection efficiencies is in general non-negligible. It seems that when dealing with aerosol particles/clusters in the sub-3 nm size range the chemical composition of the clusters and the purity of the sample have a significant impact on the detection efficiencies. The fact that a range of cut-off diameters exists and that the shapes of the detection efficiency curves are different makes it more difficult to determine the formation/nucleation/growth rates unambiguously, since it is not obvious which cut-off diameter to choose, if a calibration with exactly the same particle composition is not possible.

4.2 Evaluation of the diffusional losses in a laminar flow CPC

The design of the ultrafine TSI 3776 with its rather low aerosol flow rate inside the capillary (50 $cm^3 min^{-1}$, see Fig. 1) indicates that it has non-negligible internal losses. In addition, the comparison of the cut-off curves for the DEG CPCs and the PSMs underline this assumption. From Fig. 7 it can be seen that the PSM 1/2 have steeper slopes in the detection efficiencies and reach an efficiency close to 100 % at smaller sizes earlier than the DEG CPCs, which might be due to the fact that the DEG CPCs have larger internal losses. Another effect that might influence the shape of the detection efficiency curve could be an inhomogeneous profile of the saturation ratio inside the instrument. In the turbulent mixing type CPC, the supersaturation is not only achieved almost immediately after the mixing section, but will also be roughly the same everywhere inside the CPC, depending on the turbulence intensity. The laminar flow CPC on the other hand establishes a saturation profile with a maximum in the center of the flow. Particles travelling closer to the wall of the tube will not experience the same supersaturation as the particles in the center. Therefore those particles might be activated with a lower efficiency (Stratmann et al., 1994).

To quantify the effect of the internal losses, a set of measurements was carried out. The setup used is shown in Fig. 3d and consists of an aerosol generator (tube furnace with sodium chloride) and a Grimm nano-DMA for classification of the particles.

AMTD
6, 2151–2181, 2013

Behind the DMA, a three-way valve is located where the flow is directed either to the DEG stage or to a flexible conductive tubing before being sampled to the CPC. The tube length was adjusted until the CPC showed the same concentrations no matter whether the aerosol was going through the DEG stage or through the tube. To determine the final effective tube length, the length of the condenser was estimated (8 cm). This has to be subtracted from the total length, since the particles at this stage can be considered big enough not to be substantially affected by diffusional losses any more. Prior to these measurements the DEG CPC was dried carefully and the saturator temperature was set to 30 °C to avoid any activation of the particles. This way, the effective length was evaluated to be 19 cm at a flow rate of 0.3 L min^{-1} through the tube. Figure 8 shows the calculated penetration efficiencies according to Gormley and Kennedy (1948) for the size range 1–10 nm using the experimentally determined tube length and flow rate. The detection efficiencies, applying these corrections of the DEG CPC 1 (red symbols) and the uncorrected points (green symbols) are shown in Fig. 9. The fact that the 100 % efficiency line is reached for particles larger than 3 nm indicates that the corrections applied are appropriate. As a comparison the data points from the PSM 2 for the positively charged sodium chloride clusters are added to this figure (black symbols). It shows that after correcting for the internal losses, the slopes of the detection efficiency curves of the laminar-flow CPC are comparable to the mixing-type CPCs, in which the diffusional losses of particles are considerably lower. Thus the red symbols (corrected data) are representing the activation efficiency of particles in the DEG CPC 1.

As the internal losses are rather significant (approx. 50 % at 2 nm), it needs to be discussed in how far the results from DEG CPC measurements such as the nucleation and formation rates corrections have to be applied to account for these internal losses. However the same applies to all continuous-flow CPCs when measuring close to their cut-off sizes. Usually it is not possible to correct the data without knowing the exact size distribution of the measured particles, because the diffusional losses are

AMTD
6, 2151–2181, 2013

size dependent. Therefore, in our data analysis, the uncorrected detection efficiency is used.

4.3 Ambient measurements

In this section measurements of outdoor air in Helsinki (in Kumpula university campus area, ca. 4 km from Helsinki city center) as well as indoor air from the aerosol laboratory, are shown. The left hand side of Fig. 10 shows the comparison of total particle concentration measured with the DEG CPC 2 and the PSM 1 in scanning mode, measuring lab air for a time period of approximately 10 h. The different colors of the lines represent the different flow settings for the saturator flows of the PSM. The right half of the figure shows outdoor air measurements. The two channels with the highest mixing ratios (lowest cut-off diameter) of the PSM (green and blue line) are showing a slightly higher concentration than the other channels, especially when the overall particle concentration was low, leading to a lower condensation sink for small particles. The difference in concentration between the flow settings was larger in the indoor air measurements, which might be due to the fact that lots of small particles were present in the laboratory air as the aerosol generation setup was running. It is worth noting that all the settings of the scanning PSM show very similar concentrations during the outdoor air measurements. Therefore it can be concluded that no significant amount of nucleation mode particles was present during this measurement period. The sudden increase of the particle concentration around 04:30 UTC (06:30 LT – local time) might be due to the beginning of the morning traffic, as the measurement place is close to a big road. In the inset of the figure a scatter plot shows the correlation between the total concentrations measured by the DEG CPC and the PSM during the ambient measurement period. It shows a good agreement (R^2 = 0.95) between the DEG CPC 2 (d_{50} = 1.5–1.8 nm) and the 0.55 L min^{-1} setting (d_{50} = 1.5 nm) of the scanning PSM.

AMTD
6, 2151–2181, 2013

5 Conclusions

We investigated the performance of CPCs which are sensitive to particles below 3 nm in mobility equivalent diameter. Four different ultrafine CPCs which all use diethylene glycol as the working fluid were studied. A variety of calibration measurements using different methods of generating test aerosols were performed.

The determination of the exact detection efficiency functions of the CPCs, is important when measuring concentrations close to the cut-off sizes. If the cut-off function is shallow, both the nucleation rates and the growth rates can be affected by the shape of the detection efficiency curves. Our results show that the 50 % detection efficiencies of the diethylene glycol based particle counters differed depending on the composition of the particles. In the laboratory this is not a problem as there the particle composition is typcially known, but in the real atmosphere the composition is unknown. This leads to a higher uncertainty in the data obtained with the atmospheric nanoparticles.

The CPCs capable of detecting particles in the range of 1 to 2 nm are highly important when studying atmospheric nucleation because the corrections for calculating the "true" nucleation rates are considerably reduced and information about particle growth rates in the size range between 1 and 3 nm can be obtained. Also seemingly redundant measurements with multiple sub-3 nm CPCs are highly useful, since matching data from several CPCs with independent operating principles adds greatly to the confidence in the measurements, allows a rapid and reliable determination of data quality and helps to identify any instrumental problems. When comparing the mixing type CPCs with the laminar-flow DEG CPCs, they agree fairly well based on our experiments. The measurements at CLOUD have underlined the good agreement of the two counter types and the importance of using low cut-off counters for the nucleation measurements (Kirkby et al., 2011).

Acknowledgements. We would like to thank CERN for supporting CLOUD with important technical and financial resources, and for providing a particle beam from the CERN Proton Synchrotron. This research has received funding from the EC Seventh Framework Programme

AMTD
6, 2151–2181, 2013

(Marie Curie Initial Training Network “CLOUD-ITN” grant no. 215072, and ERC-Advanced “ATMNUCLE” grant no. 227463), the German Federal Ministry of Education and Research (project no. 01LK0902A), the Academy of Finland Center of Excellence program (project no. 1118615). We like to thank Sebastian Ehrhart, Linda Rondo and Bertram Bühner for fruitful discussions.

References

Chen, D. R. and Pui, D. H. Y.: Numerical and experimental studies of particle deposition in a tube with a conical contraction – laminar flow regime, in: Aerosol Measurement, John Wiley and Sons Inc., New York, 173–176, 2001. 2160

Ehn, M., Junninen, H., Schobesberger, S., Manninen, H. E., Franchin, A., Sipilä, M. M., Petäjä, T., Kerminen, V.-M., Tammet, H., Mirme, A., Mirme, S., Horrak, U., Kulmala, M., and Worsnop, D. R.: An instrumental comparison of mobility and mass measurements of atmospheric small ions, Aerosol Sci. Tech., 45, 522–532, 2011. 2159

Fernandez de la Mora, J., Thomson, B. A., and Gamero-Castaño, M.: Tandem mobility mass spectrometry study of electrosprayed tetraheptyl ammonium bromide clusters, J. Am. Soc. Mass. Spectrom., 16, 717–732, 2005. 2159

Gormley, P. G. and Kennedy, M.: Diffusion from a stream flowing through a cylindrical tube, in: Proceedings of the Royal Irish Academy, Section A: Mathematical and Physical Sciences, 52, available at: http://www.jstor.org/stable/20488498 last access: January 2013, University College Dublin, 163–169, 1948. 2164

Herrmann, W., Eichler, T., Bernardo, N., and Fernandez de la Mora, J.: Turbulent transition arises at Reynolds number 35 000 in a short ViennaType DMA with a large laminarization inlet, in: AAAR, Annual Conference, St. Louis, Minnesota, USA, 2000. 2159

Iida, K., Stolzenburg, M. R., and McMurry, P. H.: Effect of working fluid on sub-2 nm particle detection with a laminar flow ultrafine condensation particle counter, Aerosol Sci. Tech., 43, 81–96, 2009. 2154, 2156, 2161, 2162

Jiang, J., Attoui, M., Heim, M., Brunelli, N. A., McMurry, P. H., Kasper, G., Flagan, R. C., Giapis, K., and Mouret, G.: Transfer functions and penetrations of five differential mobility analyzers for sub-2 nm particle classification, Aerosol. Sci. Tech., 45, 480–492, 2011a. 2160

AMTD
6, 2151–2181, 2013

Jiang, J., Zhao, J., Chen, M., Eisele, F. L., Scheckman, J., Williams, B. J., Kuang, C., and McMurry, P. H.: First measurements of neutral atmospheric cluster and 1–2 nm particle number size distributions during nucleation events, Aerosol Sci. Tech., 45, 2–5, 2011b. 2155

Junninen, H., Ehn, M., Petäjä, T., Luosujärvi, L., Kotiaho, T., Kostiainen, R., Rohner, U., Gonin, M., Fuhrer, K., Kulmala, M., and Worsnop, D. R.: A high-resolution mass spectrometer to measure atmospheric ion composition, Atmos. Meas. Tech., 3, 1039–1053, doi:10.5194/amt-3-1039-2010, 2010. 2159

Kangasluoma, J., Junninen, H., Lehtipalo, K., Sipilä, M., Mikkilä, J., Vanhanen, J., Attoui, M., Worsnop, D., Kulmala, M., and Petäjä, T.: Remarks on ion generation for CPC calibrations in the sub 3 nm size range, Aerosol Sci. Tech., doi:10.1080/02786826.2013.773393, in press, 2013. 2162

Ki Ku, B. and Fernandez de la Mora, J.: Relation between electrical mobility, mass, and size for nanodrops 1–6.5 nm in diameter in air, Aerosol Sci. Tech., 43, 241–249, 2009. 2159

Kirkby, J., Curtius, J., Almeida, J., Dunne, E., Duplissy, J., Ehrhart, S., Franchin, A., Gagne, S., Ickes, L., Kürten, A., Kupc, A., Metzger, A., Riccobono, F., Rondo, L., Schobesberger, S., Tsagkogeorgas, G., Wimmer, D., Amorim, A., Bianchi, F., Breitenlechner, M., David, A., Dommen, J., Downard, A., Ehn, M., Flagan, R. C., Haider, S., Hansel, A., Hauser, D., Jud, W., Junninen, H., Kreissl, F., Kvashin, A., Laaksonen, A., Lehtipalo, K., Lima, J., Lovejoy, E. R., Makhmutov, V., Mathot, S., Mikkilä, J., Minginette, P., Mogo, S., Nieminen, T., Onnela, A., Pereira, P., Petäjä, T., Schnitzhofer, R., H. Seinfeld, J., Sipilä, M., Stozhkov, Y., Stratmann, F., Tome, A., Vanhanen, J., Viisanen, Y., Vrtala, A., Wagner, P. E., Walther, H., Weingartner, E., Wex, H., Winkler, P. M., Carslaw, K. S., Worsnop, D. R., Baltensperger, U., and Kulmala, M.: Role of sulphuric acid, ammonia and galactic cosmic rays in atmospheric aerosol nucleation, Nature, 476, 429–433, 2011. 2155, 2166

Kuang, C., Chen, M., McMurry, P. H., and Wang, J.: Modification of laminar flow ultrafine condensation particle counters for the enhanced detection of 1 nm condensation nuclei, Aerosol Sci. Tech., 46, 309–315, 2011. 2157, 2162

Kulmala, M., Mordas, G., Petäjä, T., Grönholm, T., Aalto, P. P., Vehkamäki, H., Hienola, A. I., Herrmann, E., Sipilä, M., Riipinen, I., Manninen, H. E., Hämeri, K., Stratmann, F., Bilde, M., Winkler, P. M., Birmili, W., and Wagner, P. E.: The condensation particle counter battery (CPCB): a new tool to investigate the activation properties of nanoparticles, J. Aerosol Sci., 38, 289–304, 2007a. 2154

AMTD
6, 2151–2181, 2013

Kulmala, M., Riipinen, I., Sipilä, M., Manninen, H. E., Petäjä, T., Junninen, H., Dal Maso, M., Mordas, G., Mirme, A., Vana, M., Hirsikko, A., Laakso, L., Harrison, R. M., Hanson, I., Leung, C., Lehtinen, K. E. J., and Kerminen, V.-M.: Toward direct measurement of atmospheric nucleation, Science, 318, 89–92, 2007b. 2154

Kulmala, M., Petäjä, T., Nieminen, T., Sipilä, M., Manninen, H. E., Lehtipalo, K., Dal Maso, M., Aalto, P., Junninen, H., Paasonen, P., Riipinen, I., Lehtinen, K., Laaksonen, A., and Kerminen, V. M.: Measurement of the nucleation of atmospheric aerosol particles, Nat. Protoc., 7, 1651–1667, 2012. 2153

Lehtipalo, K., Sipilä, M., Riipinen, I., Nieminen, T., and Kulmala, M.: Analysis of atmospheric neutral and charged molecular clusters in boreal forest using pulse-height CPC, Atmos. Chem. Phys., 9, 4177–4184, doi:10.5194/acp-9-4177-2009, 2009. 2154

Lehtipalo, K., Kulmala, M., Sipilä, M., Petäjä, T., Vana, M., Ceburnis, D., Dupuy, R., and O'Dowd, C.: Nanoparticles in boreal forest and coastal environment: a comparison of observations and implications of the nucleation mechanism, Atmos. Chem. Phys., 10, 7009–7016, doi:10.5194/acp-10-7009-2010, 2010. 2154

McMurry, P. H.: The history of condensation nucleus counters, Aerosol Sci. Tech., 33, 297–322, 2000. 2153

Merikanto, J., Spracklen, D. V., Mann, G. W., Pickering, S. J., and Carslaw, K. S.: Impact of nucleation on global CCN, Atmos. Chem. Phys., 9, 8601–8616, doi:10.5194/acp-9-8601-2009, 2009. 2153

Middlebrook, A. M., Thomson, D. S., and Murphy, D. M.: On the purity of laboratory-generated sulfuric acid droplets and ambient particles studied by laser mass spectrometry, Aerosol Sci. Tech., 27, 293–307, 1997. 2158

Mordas, G., Kulmala, M., Petäjä, T., Aalto, P. P., Matulevicius, V., Grigoraitis, V., Ulevicius, V., Grauslys, V., Ukkonen, A., and Hämeri, K.: Design and performance characteristics of a condensation particle counter UF-02proto, Boreal Environ. Res., 10, 543–552, 2005. 2154

Saghafifar, H., Kürten, A., Curtius, J., von der Weiden, S.-L., Hassanzadeh, S., and Borrmann, S.: Characterization of a modified expansion condensation particle counter for detection of nanometer-sized particles, Aerosol Sci. Tech., 43, 767–780, 2009. 2154

Scheibel, H. G. and Porstendörfer, J.: Generation of monodisperse Ag- and NaCl-aerosols with particle diameters between 2 and 300 nm, J. Aerosol Sci., 14, 113–126, 1983. 2158

AMTD
6, 2151–2181, 2013

Seto, T., Okuyama, K., de Juan, L., and Fernandez de la Mora, J.: Condensation of supersaturated vapors on monovalent and divalent ions of varying size, J. Chem. Phys., 107, 1576–1585, 1997. 2154

Sgro, L. A. and Fernandez de la Mora, J.: A simple turbulent mixing CNC for charged particle detection down to 1.2 nm, Aerosol Sci. Tech., 38, 1–11, 2004. 2154

Sipilä, M., Lehtipalo, K., Kulmala, M., Petäjä, T., Junninen, H., Aalto, P. P., Manninen, H. E., Kyrö, E.-M., Asmi, E., Riipinen, I., Curtius, J., Kürten, A., Borrmann, S., and O'Dowd, C. D.: Applicability of condensation particle counters to measure atmospheric clusters, Atmos. Chem. Phys., 8, 4049–4060, :doi10.5194/acp-8-4049-2008, 2008. 2154

Sipilä, M., Lehtipalo, K., Attoui, M., Neitola, K., Petäjä, T., Aalto, P. P., O'Dowd, C. D., and Kulmala, M.: Laboratory verification of PH-CPC's ability to monitor atmospheric sub-3 nm clusters, Aerosol Sci. Tech., 43, 126–135, 2009. 2154, 2162

Sipilä, M., Berndt, T., Petäjä, T., Brus, D., Vanhanen, J., Stratmann, F., Patokoski, J., Mauldin III, R. L., Hyvärinen, A.-P., Lihavainen, H., and Kulmala, M.: The role of sulfuric acid in atmospheric nucleation, Science, 327, 1243–1246, 2010. 2153

Stolzenburg, M. R. and McMurry, P. H.: An ultrafine aerosol condensation nucleus counter, Aerosol Sci. Tech., 14, 48–65, 1991. 2153, 2154

Stratmann, F., Otto, E., and Fissan, H.: Thermophoretical and diffusional particle transport in cooled laminar tube flow, J. Aerosol Sci., 25, 1305–1319, doi:10.1016/0021-8502(94)90127-9, 1994. 2160, 2163

Vanhanen, J., Mikkilä, J., Lehtipalo, K., Sipilä, M., Manninen, H. E., Siivola, E., Petäjä, T., and Kulmala, M.: Particle size magnifier for Nano-CN detection, Aerosol Sci. Tech., 45, 533–542, 2011. 2154, 2155, 2156, 2158

Wehner, B., Siebert, H., Hermann, M., Ditas, F., and Wiedensohler, A.: Characterisation of a new Fast CPC and its application for atmospheric particle measurements, Atmos. Meas. Tech., 4, 823–833, doi:10.5194/amt-4-823-2011, 2011. 2160, 2161, 2175

Winkler, P. M., Steiner, G., Vrtala, A., Vehkamäki, H., Noppel, M., Lehtinen, K. E. J., Reischl, G. P., Wagner, P. E., and Kulmala, M.: Heterogeneous nucleation experiments bridging the scale from molecular ion clusters to nanoparticles, Science, 319, 1374–1377, 2008. 2154, 2162

AMTD
6, 2151–2181, 2013

Table 1. Summary of the 50 % detection efficiencies of the four CPCs for different types of aerosols. When using tungsten oxide as test aerosol the smallest size that can be produced was about 1.5 nm, where the PSMs still detected roughly 60 %.

type of aerosol	polarity	d_{50} DEG CPC 1	d_{50} DEG CPC 2	d_{50} PSM1	d_{50} PSM2
sulphuric acid	negative	2.0 nm	no data	no data	no data
tungsten oxide	negative	2.0 nm	no data	< 1.5 nm	< 1.5 nm
tungsten oxide	positive	2.0 nm	no data	< 1.5 nm	< 1.5 nm
ammonium sulphate	negative	1.4 nm	1.4 nm	1.2 nm	1.1 nm
ammonium sulphate	positive	no data	1.8 nm	1.6 nm	1.6 nm
sodium chloride	negative	1.7 nm	1.5 nm	1.2 nm	1.2 nm

AMTD
6, 2151–2181, 2013

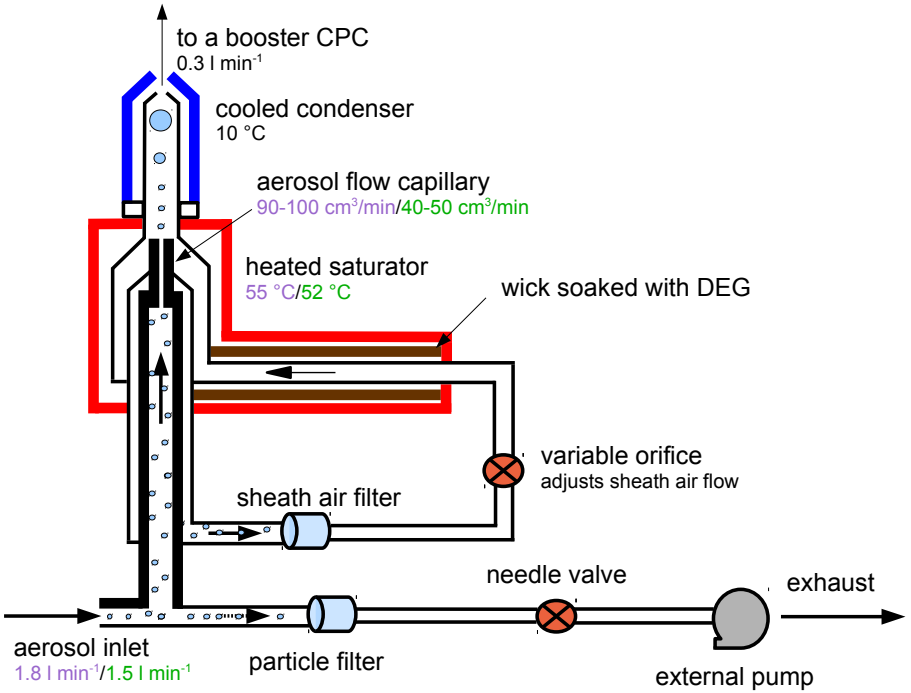

Fig. 1. A detailed overview of the setup for DEG CPC 1 and 2. The setup is based on the commercially available TSI 3776. For the DEG CPC 2 a valve and a pump were added to give the possibility to increase the inlet flow. The flow and temperature settings for each CPC are shown in magenta for the DEG CPC 2 and in green the DEG CPC 1.

AMTD
6, 2151–2181, 2013

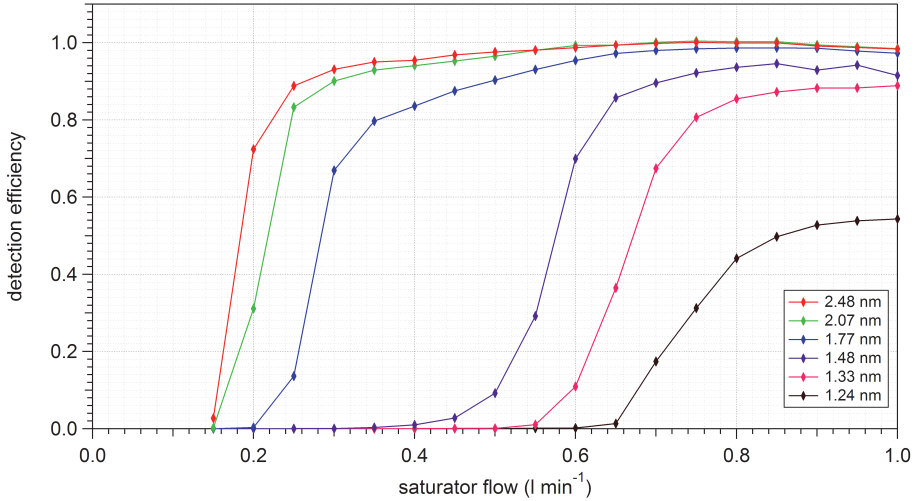

Fig. 2. Detection efficiency of the PSM as a function of the saturator flow rate for negatively charged ammonium sulphate particles at different sizes. The different lines are measurements with differently sized particles and determine the saturator flow rate which is needed for achieving the according cut-off diameters.

AMTD
6, 2151–2181, 2013

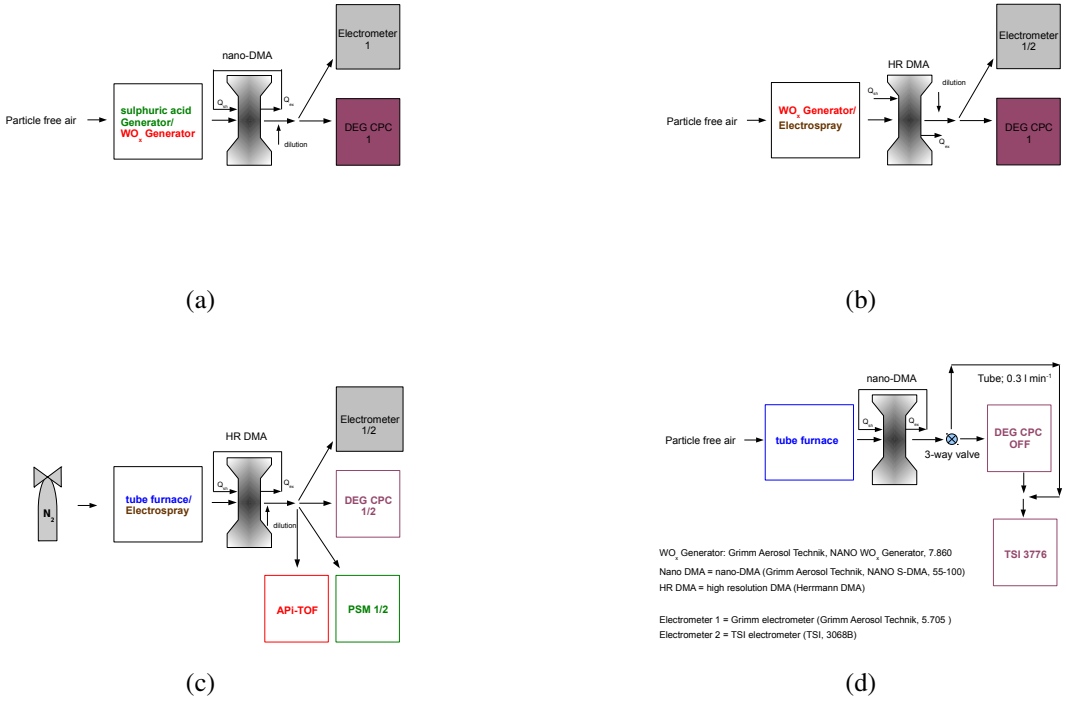

Fig. 3. Overview of the different configurations used for the calibrations. The aerosol generators used together with the nano-DMA are shown in **(a)**. The measurement configurations using the high resolution DMA in the open loop mode are shown in **(b)** and for the closed loop mode in **(c)**; **(d)** shows the setup for quantifying the internal losses of the DEG CPCs.

AMTD
6, 2151–2181, 2013

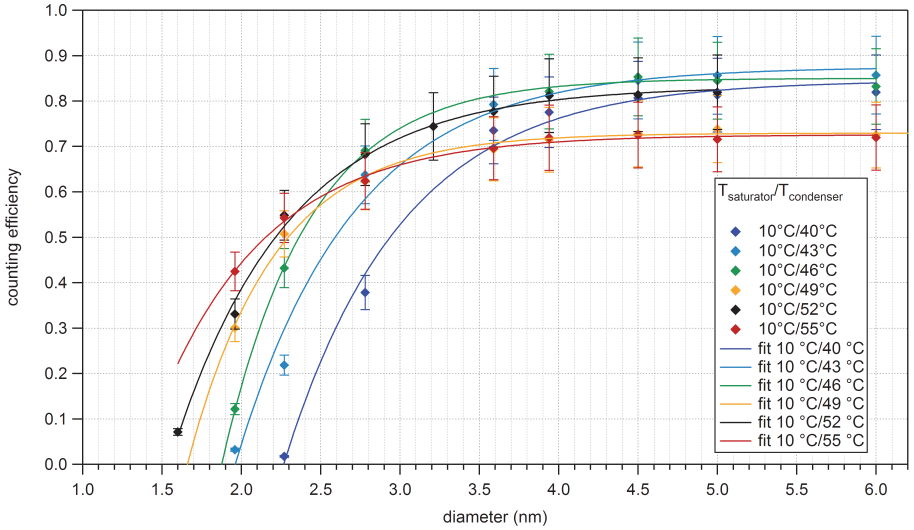

Fig. 4. Detection efficiencies for DEG CPC 1 at different temperature settings, using tungsten oxide particles. The condenser temperature was 10 °C and the saturator temperature was varied from 40 °C (blue) up to 55 °C (red). The black symbols show the setting of 52 °C, which was used throughout all the experiments shown in this work. The fit curves to the data are based on the parameterization by Wehner et al. (2011).

AMTD
6, 2151–2181, 2013


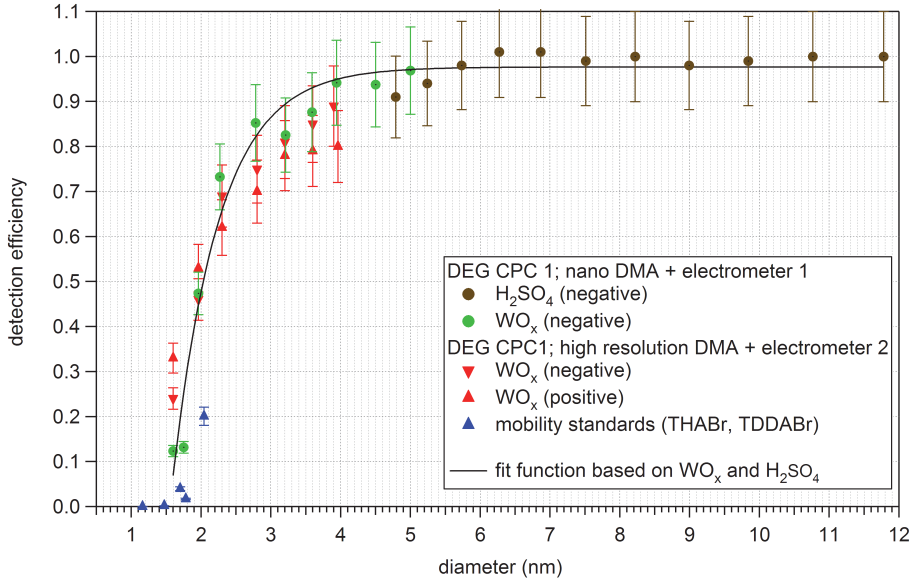

Fig. 5. Detection efficiencies for the DEG CPC 1 for different particle types of both polarities classified with a nano-DMA and a high resolution DMA in open loop. For particles larger than 5 nm, sulphuric acid was used as test-aerosol. Mobility standards are not included for the fit.

AMTD
6, 2151–2181, 2013

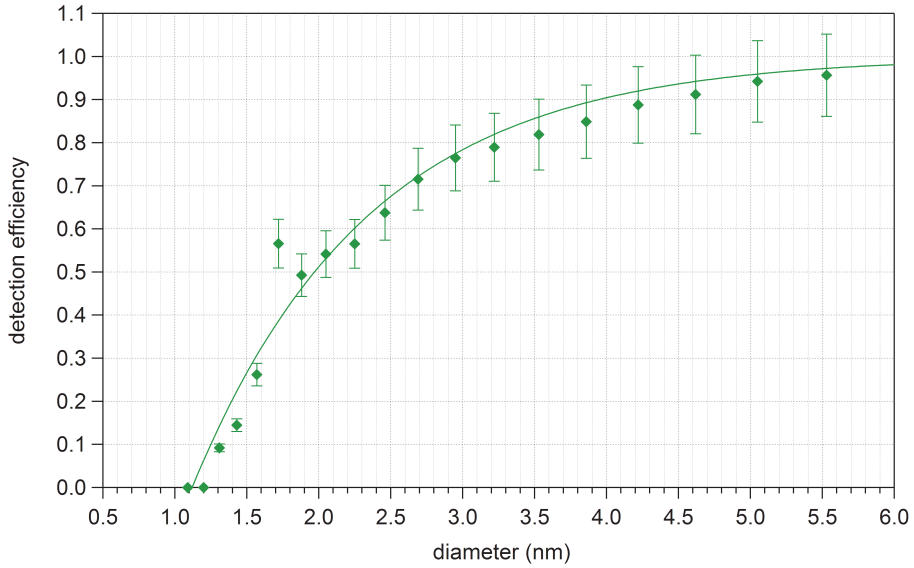

Fig. 6. Detection efficiencies for the DEG CPC 1 using negatively charged sulphuric acid particles classified with a nano-DMA.

AMTD
6, 2151–2181, 2013

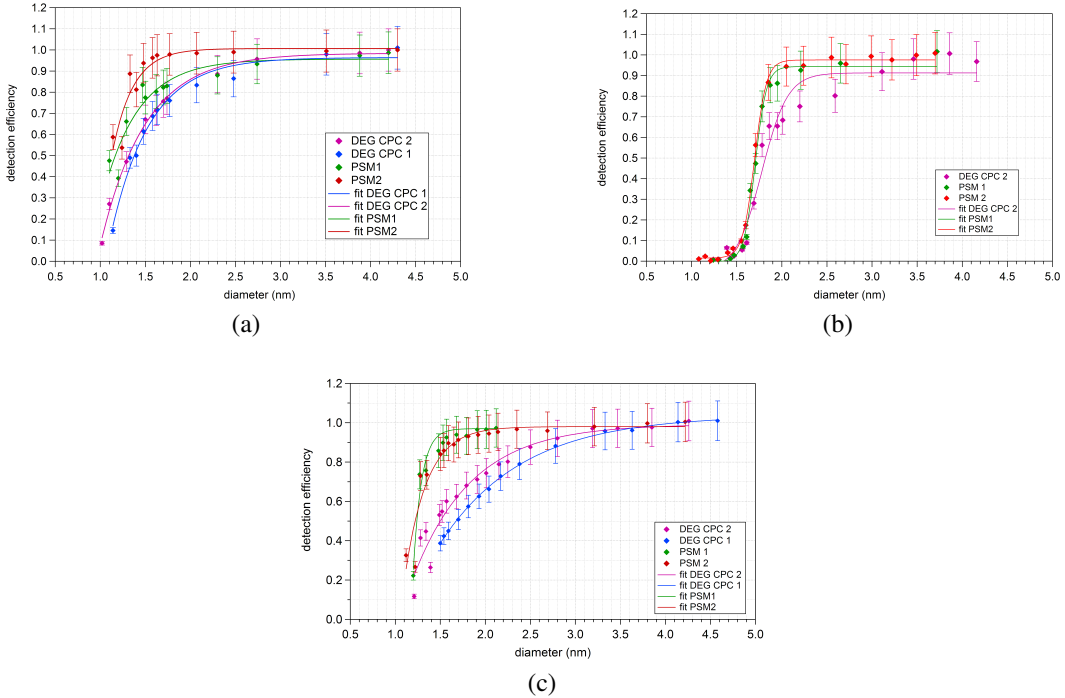

Fig. 7. Detection efficiencies for the DEG CPCs compared to the PSMs using negatively charged ammonium sulphate **(a)**, positively charged ammonium sulphate **(b)** and negatively charged sodium chloride particles **(c)** produced in the closed loop high resolution setup.

AMTD
6, 2151–2181, 2013

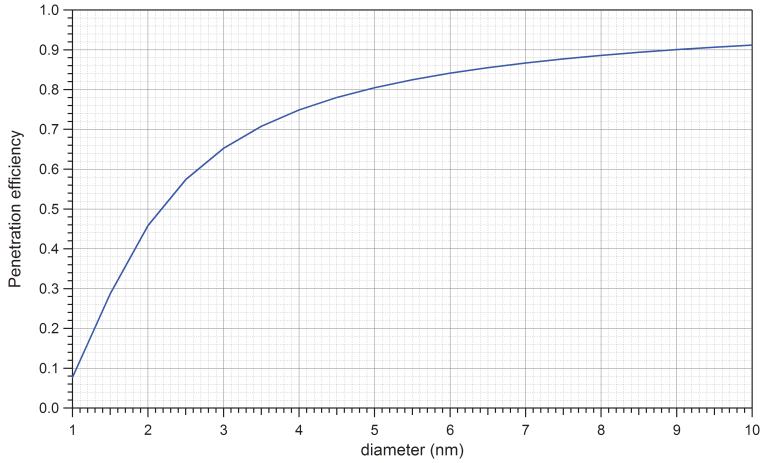

Fig. 8. Calculated penetration efficiencies as a function of size for the experimentally determined parameters (flow rate and tube length). They were derived by measuring the concentrations of size selected aerosols (3, 4 and 6 nm) once after passing a flexible tube and once after passing through an empty laminar flow CPC.

AMTD
6, 2151–2181, 2013

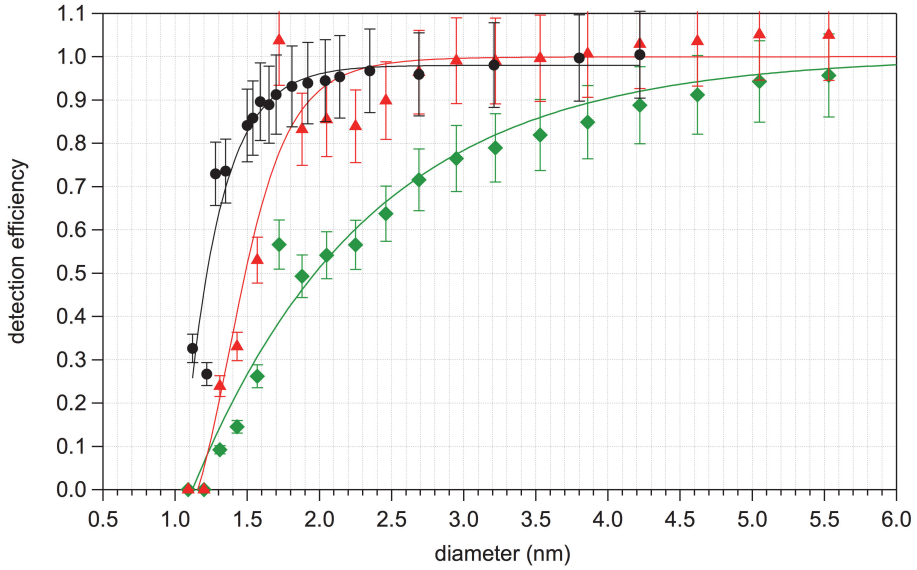

Fig. 9. Detection efficiencies of DEG CPC 1 before correcting for internal losses (green symbols) and after the correction (red symbols). As a comparison the (uncorrected) data from the PSM 2 from Fig. 7c is shown here in black.

AMTD
6, 2151–2181, 2013

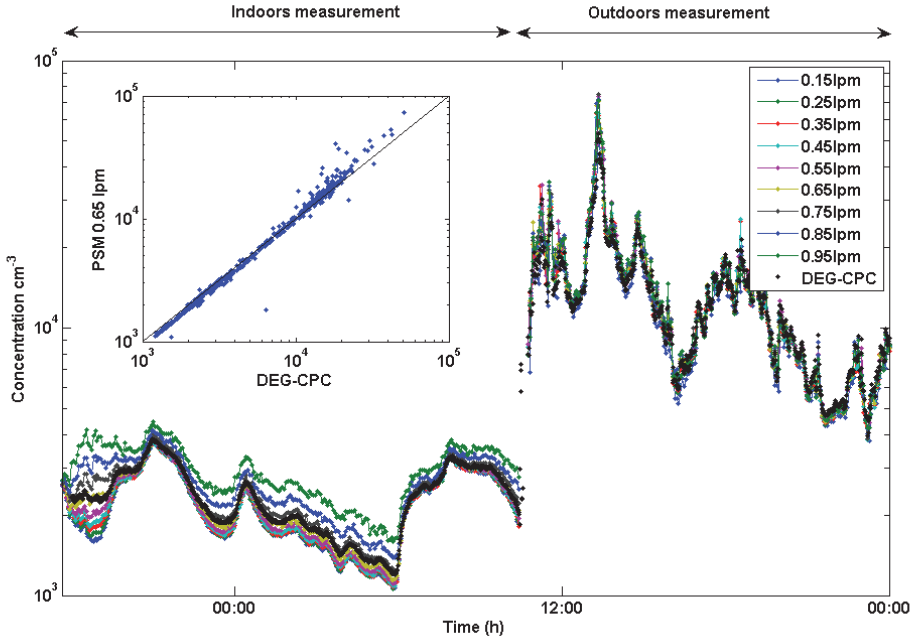

Fig. 10. Comparison of the scanning PSM and DEG CPC 1 measuring the total particle concentration indoors and outdoors. The different coloured lines for the scanning PSM show the different flow rate settings for the saturator flow. The scatter plot shows the correlation between the 0.55 L min^{-1} saturator flow setting for the scanning PSM and the DEG CPC 1.

AMTD
6, 2151–2181, 2013